Laser-excited motion of liquid crystals confined in a microsized volume with a free surface

A. V. Zakharov[*]

Saint Petersburg Institute for Machine Sciences, the Russian Academy of Sciences, Saint Petersburg 199178, Russia

P. V. Maslennikov[†]

Immanuel Kant Baltic Federal University, Kaliningrad 236040, Str. Universitetskaya 2, Russia

The thermally excited vortical flow in a microsized liquid crystal (LC) volume with a free LC-air interface has been investigated theoretically based on the nonlinear extension of the Ericksen-Leslie theory, with accounting the entropy balance equation. Analysis of the numerical results show that due to interaction between the gradients of the director field $\nabla \hat{\mathbf{n}}$ and temperature field ∇T, caused by the focused heating, the thermally excited vortical fluid flow is maintained in the vicinity of the heat source. Calculations show that the magnitude and direction of the velocity field $\mathbf{v}$, as well as the height of the LC-air interface are influenced by the depth of the heat penetration in the LC volume. It has been shown that there is the point in the vicinity of the LC-air interface where the thermally excited vortical flow changes the direction from anticlockwise to clockwise.

I. INTRODUCTION

The manipulation of tiny amounts of molecular liquids has become a paradigm in various fields of applied chemistry-, physics-, and biotechnology-related microfluidics. The decreasing of cell sizes down to nano(micro)-level provides a close connection of liquid crystals (LCs) model with biological liquid [1]. The development of future biodynamics applications requires complicated investigation of natural anisotropic soft materials with multicoupling interactions of inner fields initiated by external forces. The problem of motion of an ultrathin (a few microliters) LC drops confined in the microsized volume, under the influence of the temperature gradient, caused, for instance, by the laser beam, has drawn considerable attention [2–5]. The understanding of how the LC material deforms under the influence of the temperature gradient is a question of great fundamental interest, as well as an essential piece of knowledge in soft material science. Despite the fact that certain qualitative and quantitative advances in a hydrodynamic description of the relaxation processes in the LC phase under the influence of the temperature gradient have been achieved, it is still too early to talk about the development of a theory that would make it possible to describe the dissipation processes in confined LC phase with a free upper LC-air interface under the influence of the temperature gradient ∇T [3,4]. Thus, we are primarily concerned here on describing how the temperature gradient caused by induced heating in the interior of the microsized hybrid-aligned LC (HALC) volume with a free upper LC-air interface can produce the hydrodynamic flow and, as a result, how it can deform the free LC-air interface [5]. This problem will be treated in the framework of the appropriate nonlinear extension of the Ericksen-Leslie theory [6,7], with accounting the thermoconductivity equation for the temperature field T [8,9].

The present paper is organized as follows: the relevant equations describing the director motion, fluid flow, and temperature distribution in the above-named system are given in Sec. II; numerical results for possible hydrodynamic regimes are given in Sec. III; conclusions are summarized in Sec. IV.

II. FORMULATION OF THE BALANCE OF THE MOMENTUM, TORQUE, AND CONDUCTIVITY EQUATIONS FOR NEMATIC FLUIDS

In this paper, we consider the dynamics of free and initially flat LC-air interface under the influence of the temperature gradient ∇T, caused by the focused heating. Thus, we are concerned here with describing how the temperature gradient, caused by induced heating in the interior of the microsized hybrid- aligned LC (HALC) volume with a free upper LC-air interface, can produce the hydrodynamic flow $\mathbf{v}$ and, as a result, how it can deform the free LC-air interface. We consider the HALC cell delimited by one lower horizontal solid surface, located at $z = -d$, one upper free flat LC-air interface, initially located at $z = d$, and two lateral solid surfaces at distance $2L$ on scale on the order of micrometers. The coordinate system defined by our task assumes that the director $\hat{\mathbf{n}} = n_x \hat{\mathbf{i}} + n_z \hat{\mathbf{k}}$ is in the XZ plane, where $\hat{\mathbf{i}}$ is the unit vector directed parallel to the lower restricted surface, which, in turn, coincides with the planar director orientation on the lower restricted surface ($\hat{\mathbf{i}} \parallel \hat{\mathbf{n}}_{z=-d}$), whereas the unit vector $\hat{\mathbf{k}}$ is directed parallel to the lateral restricted surfaces, which coincides with the planar director orientation on these surfaces ($\hat{\mathbf{k}} \parallel \hat{\mathbf{n}}_{x=\pm L}$), and $\hat{\mathbf{j}} = \hat{\mathbf{k}} \times \hat{\mathbf{i}}$. Therefore, the hybrid aligned nematic phase contains a gradient of $\nabla \hat{\mathbf{n}}$ from planar orientation on the lower and both lateral surfaces to homeotropic orientation on the upper free LC-air interface Γ, i.e.,

$$(n_x)_{x=\pm L, -d < z < d} = 0,$$
$$(n_x)_{-L < x < L, z=-d} = 1, \quad (1)$$
$$(\vec{n} \cdot \vec{v})_\Gamma = -1.$$

Here $\vec{v} = [-\frac{H_x}{\sqrt{H_x^2+1}}, 1]$ is the normal to the free LC-air interface Γ at any time and is directed from the nematic phase

---

[*]Author to whom correspondence should be addressed: alexandre.zakharov@yahoo.ca; www.ipme.ru

[†]pashamaslennikov@mail.ru

into air, $H(x,t)$ is the height of the LC film on the top of the smooth surface, and $H_x = \frac{\partial H}{\partial x}$. We consider the temperature regime without the heat flow $\vec{q}$ across the free LC-air interface Γ

$$(\vec{q} \cdot \vec{v})_\Gamma = 0, \tag{2}$$

whereas on the rest boundaries the temperature is kept constant,

$$T_{-L<x<L, z=-d} = T_{x=\pm L, -d<z<d} = T_0. \tag{3}$$

We will assume the no-slip boundary conditions for the nematogenic molecules on these solid bounding surfaces, i.e.,

$$\mathbf{v}_{-L<x<L, z=-d} = \mathbf{v}_{x=\pm L, -d<z<d} = \mathbf{0}, \tag{4}$$

where $\mathbf{v} = u\hat{\mathbf{i}} + w\hat{\mathbf{k}}$ is the velocity vector with the horizontal $u \equiv v_x(x,z,t)$ and vertical $w \equiv v_z(x,z,t)$ components. The bounding condition for the velocity on the upper free LC-air interface Γ can be obtained from the linear balance equation transmitted to the surface Γ. In our case, that balance leads to the tangential,

$$[\vec{v} \cdot \sigma \cdot \vec{t}]_\Gamma = 0, \tag{5}$$

and normal,

$$[\vec{v} \cdot \sigma \cdot \vec{v}]_\Gamma = 2\gamma\kappa, \tag{6}$$

force balances, where $\vec{t} = [1, \frac{H_x}{\sqrt{H_x^2+1}}]$ is an additional unit tangent vector, γ is the LC-air surface tension, $\kappa = \frac{H_{xx}}{\sqrt{1+H_x^2}}$ is the curvature of free LC-air interface Γ at any time, and σ is the full stress tensor (ST). Taking into account the microsized HALC volume, one can assume the mass density ρ to be constant across the sample, and thus deal with an incompressible fluid. The incompressibility condition $\nabla \cdot \mathbf{v} = 0$ assumes that

$$u_x + w_z = 0, \tag{7}$$

where $u_x = \frac{\partial u}{\partial x}$, and $w_z = \frac{\partial w}{\partial z}$.

The hydrodynamic equations describing the reorientation of the LC phase in 2D case, when the system is subjected to a temperature gradient ∇T, due to uniform heat flow $\mathbf{q}$, can be derived from the torque balance equation

$$\mathbf{T}_{el} + \mathbf{T}_{vis} + \mathbf{T}_{tm} = \mathbf{0}, \tag{8}$$

where [3,4] $\mathbf{T}_{el} = \frac{\delta\mathcal{W}_{el}}{\delta\hat{\mathbf{n}}} \times \hat{\mathbf{n}}$ is the elastic, $\mathbf{T}_{vis} = \frac{\delta\mathcal{R}^{vis}}{\delta\hat{\mathbf{n}}_t} \times \hat{\mathbf{n}}$ is the viscous, and $\mathbf{T}_{tm} = \frac{\delta\mathcal{R}^{tm}}{\delta\hat{\mathbf{n}}_t} \times \hat{\mathbf{n}}$ is the thermomechanical torques, respectively (for details, see the Appendix). The linear momentum equation for the velocity field $\mathbf{v}$ can be written as

$$\rho \frac{d\mathbf{v}}{dt} = \nabla \cdot \sigma, \tag{9}$$

where $\frac{d\mathbf{v}}{dt} = \frac{\partial v}{\partial t} + uv_x + wv_z$, $\sigma = \sigma^{el} + \sigma^{vis} + \sigma^{tm} - P\mathcal{E}$ is the full ST, and $\sigma^{el} = -\frac{\partial\mathcal{W}_{el}}{\partial\nabla\hat{\mathbf{n}}} \cdot (\nabla\hat{\mathbf{n}})^T$, $\sigma^{vis} = \frac{\delta\mathcal{R}^{vis}}{\delta\nabla\mathbf{v}}$, and $\sigma^{tm} = \frac{\delta\mathcal{R}^{tm}}{\delta\nabla\mathbf{v}}$ are the ST components corresponding to the elastic, viscous, and thermomechanical forces, respectively (see the Appendix). Here, $\mathcal{R} = \mathcal{R}^{vis} + \mathcal{R}^{tm} + \mathcal{R}^{th}$ is the full Rayleigh dissipation function, $\mathcal{W}_{el} = \frac{1}{2}[K_1(\nabla \cdot \hat{\mathbf{n}})^2 + K_3(\hat{\mathbf{n}} \times \nabla \times \hat{\mathbf{n}})^2]$ denotes the elastic energy density, K_1 and K_3 are splay and bend elastic coefficients, P is the hydrostatic pressure in the

HALC system, and $\mathcal{E}$ is the unit tensor. When the temperature gradient $\nabla T(\sim 1.0 \, [\text{K}/\mu\text{m}])$ is set up, for instance, by means of the laser beam focused in the interior of the nematic volume with the free upper LC-air interface, we expect that the temperature field $T(x,z,t)$ satisfies the heat conduction equation [8],

$$\rho C_P \frac{dT}{dt} = -\nabla \cdot \mathbf{q} + O(x,z), \tag{10}$$

where $\mathbf{q} = -T\frac{\delta\mathcal{R}}{\delta\nabla T}$ denotes the heat flow in the HALC system, C_P is the heat capacity of the LC system, $O(x,z) = O_0 \exp[-2\frac{(x-x_0)^2+(z-z_0)^2}{\Delta^2}]\mathcal{H}(t_{in} - t)$ is the heat source, $\mathcal{H}(t_{in} - t)$ is the Heaviside step function, $O_0 = \frac{2}{\pi}\frac{\alpha\mathcal{V}}{\Delta^2}$ is the heat flow coefficient, α is the coefficient of absorption, $\mathcal{V}$ is the laser beam power, Δ is the Gaussian spot size, and t_{in} is the duration of the energy injection into the LC sample.

Now the dynamics of the height $H(x,t)$ of the LC-air interface under the influence of the temperature gradient can be obtained by solving the system of nonlinear partial differential Eqs. (8)–(10) with the appropriate boundary and initial conditions. Equations (5) and (6), together with the torque balance Eq. (8), transmitted to the LC-air interface, can be combined to yield equation for the height $H(x,t)$ in the form

$$\frac{\partial H}{\partial t} = w_\Gamma - u_\Gamma H_{,x}, \tag{11}$$

where u_Γ and w_Γ are the horizontal and vertical components of the velocity $\mathbf{v}$ on the LC-air interface Γ, respectively.

To observe the evolution of the director field $\hat{\mathbf{n}}(x,z,t)$ to its equilibrium orientation $\hat{\mathbf{n}}_{eq}(x,z)$ and the evolution of the velocity field $\mathbf{v}(x,z,t)$ caused by the temperature gradient, we consider the dimensionless analog of balance Eqs. (8)–(10). The dimensionless torque balance has the form

$$\begin{aligned}
n_z n_{x,\tau} &- n_x n_{z,\tau} \\
&= \delta_1[n_z\mathcal{M}_{0,x} - n_x\mathcal{M}_{0,z} + K_{31}(n_z f_z + n_x f_x)] \\
&\quad - \tfrac{1}{2}\psi_{xx}[1 + \gamma_{21}(n_x^2 - n_z^2)] - \tfrac{1}{2}\psi_{zz}[1 - \gamma_{21}(n_x^2 - n_z^2)] \\
&\quad \times 2\gamma_{21}\psi_{xz}n_x n_z + \psi_z\mathcal{N}_x + \mathcal{N}_z\psi_x + \delta_2(\chi_x\mathcal{L}_x + \chi_z\mathcal{L}_z).
\end{aligned} \tag{12}$$

The dimensionless linear momentum equation takes the form

$$\begin{aligned}
\delta_3\psi_{xz\tau} = {}& a_1\psi_{zzzz} + a_2\psi_{xzzz} + a_3\psi_{xxzz} + a_4\psi_{xxxz} \\
&+ a_5\psi_{xxxx} + a_6\psi_{zzz} + a_7\psi_{xzz} + a_8\psi_{xxz} \\
&+ a_9\psi_{xxx} + a_{10}\psi_{zz} + a_{11}\psi_{xz} + a_{12}\psi_{xx} + \mathcal{F},
\end{aligned} \tag{13}$$

whereas the dimensionless entropy balance can be written as

$$\begin{aligned}
\chi_\tau = {}& [\chi_x(\Lambda n_x^2 + n_z^2) + (\Lambda - 1)n_x n_z\chi_z]_x \\
&+ [\chi_z(\Lambda n_z^2 + n_x^2) + (\Lambda - 1)n_x n_z\chi_x]_z \\
&+ \delta_4\chi\left(\nabla \cdot \frac{\partial\mathcal{R}^{tm}}{\partial\nabla\chi}\right) + \delta_5 O(x,z,\tau) - \psi_z\chi_x + \psi_x\chi_z,
\end{aligned} \tag{14}$$

where $\tau = \frac{t}{t_T}$ is the dimensionless time, $t_T = \frac{\rho C_p d^2}{\lambda_\perp}$, $\bar{\psi} = \frac{t_T}{d^2}\psi$ is the scaled analog of the stream function ψ for the velocity field $\mathbf{v} = u\hat{\mathbf{i}} + w\hat{\mathbf{k}} = -\nabla \times \hat{\mathbf{j}}\psi$ (see the Appendix),

$\chi(x,z,\tau) = T(x,z,\tau)/T_{\mathrm{NI}}$ is the dimensionless temperature, T_{NI} is the temperature of the nematic-isotropic phase transition, $f = n_{x,z} - n_{z,x}$, $n_{z,\tau} = \frac{\partial n_z}{\partial \tau}$, $\mathcal{M}_0 = \nabla \cdot \hat{\mathbf{n}}$, $\mathcal{N}_z = n_z n_{x,z} - n_x n_{z,z}$, $\mathcal{L}_x = n_x n_{z,x} - \frac{3}{2} n_z n_{x,x} + \frac{1}{2} n_x n_{x,z}$, $\mathcal{L}_z = -n_z n_{x,z} + \frac{3}{2} n_x n_{z,z} - \frac{1}{2} n_z n_{z,x}$, $\bar{x} = \frac{x}{d}$, and $\bar{z} = \frac{z}{d}$ are dimensionless space variables. Notice that the overbars in the space variables x and z, as well as the stream function ψ have been (and will be) eliminated in the last as well as in the following equations. The function $\mathcal{F} = (\sigma_{xx}^{\mathrm{el}} + \sigma_{xx}^{\mathrm{tm}} - \sigma_{zz}^{\mathrm{el}} - \sigma_{zz}^{\mathrm{tm}})_{xz} + (\sigma_{zx}^{\mathrm{el}} + \sigma_{zx}^{\mathrm{tm}})_{zz} - (\sigma_{xz}^{\mathrm{el}} + \sigma_{xz}^{\mathrm{tm}})_{xx}$, the coefficients $a_i (i = 1,...,12)$, the functions $\sigma_{ij}^{\mathrm{tm}} (i,j = x,z)$ and $\sigma_{ij}^{\mathrm{el}} (i,j = x,z)$ are given in the Appendix. The set of parameters of the LC system are: $K_{31} = \frac{K_3}{K_1}$, $\gamma_{21} = \frac{\gamma_2}{\gamma_1}$, $\Lambda = \lambda_\parallel / \lambda_\perp$, $\delta_1 = \frac{t_T K_1}{\gamma_1 d^2}$, $\delta_2 = \frac{\rho C_p T_{\mathrm{NI}}}{\lambda_\perp} \frac{\xi}{\gamma_1}$, $\delta_3 = \frac{\rho d^2}{\gamma_1 t_T}$, $\delta_4 = \frac{\xi}{\lambda_\perp t_T}$, and $\delta_5 = \frac{2\alpha}{\pi \omega^2} \frac{d^2}{\lambda_\perp T_{\mathrm{NI}}} O_0$.

The reorientation of the director in the HALC volume confined between one solid and one free LC-air surfaces and two lateral solid surfaces, when the relaxation regime is produced by the tightly focused infrared laser heating, can be obtained by solving the system of nonlinear partial differential Eqs. (12)–(14) with the appropriate dimensionless boundary and initial conditions:

(i) *Boundary conditions at the solid surfaces:*

$$(n_x)_{x=\pm 10, -1 \leqslant z \leqslant 1} = 0, \quad (n_x)_{-10 \leqslant x \leqslant 10, z=-1} = 1,$$

$$\chi_{x=\pm 10, -1 \leqslant z \leqslant 1} = 0.97, \quad \chi_{-10 \leqslant x \leqslant 10, z=-1} = 0.97,$$

$$(\psi_{,x})_{x=\pm 10, -1 \leqslant z \leqslant 1} = (\psi_{,z})_{x=\pm 10, -1 \leqslant z \leqslant 1} = 0,$$

$$(\psi_{,x})_{-10 \leqslant x \leqslant 10, z=-1} = (\psi_{,z})_{-10 \leqslant x \leqslant 10, z=-1} = 0. \quad (15)$$

(ii) *Boundary conditions at the flexible free LC-air interface* Γ:

$$(\vec{n} \cdot \nabla \chi)_\Gamma = 0, \quad (\vec{n} \cdot \vec{v})_\Gamma = -1, \quad \hat{\mathcal{B}} \cdot \vec{\Psi} = \vec{\mathcal{C}}. \quad (16)$$

(iii) *Initial condition:*

$$\hat{\mathbf{n}}(\tau = 0, x, z) = \hat{\mathbf{n}}_{\mathrm{el}}(x,z), \quad (17)$$

where $\vec{\Psi} = (\psi_{xx}, \psi_{xz}, \psi_{zz})$, and both the matrix $\hat{\mathcal{B}}$ and vector $\vec{\mathcal{C}}$ are given in the Appendix, whereas the vector $\hat{\mathbf{n}}_{\mathrm{el}}(x,z)$ is obtained from Eq. (12), with $\psi_x = \psi_z = \chi_x = \chi_z = 0$.

Now the dimensionless height $\overline{H}(x,\tau) = H(x,\tau)/d$ of the LC cell on the top of the smooth solid substrate at any time τ can be calculated as

$$H_\tau + (\psi_x)_\Gamma + (\psi_z)_\Gamma H_x = 0, \quad (18)$$

where $w(x,\tau)_{x \in \Gamma}$ is the vertical component of the velocity vector $\mathbf{v} = u\hat{\mathbf{i}} + w\hat{\mathbf{k}} = -\nabla \times \hat{\mathbf{j}} \psi$ on the interface Γ. Notice that the overbar in the function H has been (and will be) eliminated in the last, as well as in the following equations.

Thus, when the director $\hat{\mathbf{n}}$ is strongly homeotropically anchored to the lower restricted surface and planar to the lateral restricted surfaces, the value of $\hat{\mathbf{n}}$ has to satisfy the boundary conditions Eqs. (15) and (16) and its initial orientation Eq. (17), and then, under the action of the viscous, elastic, and thermomechanical forces, allowed to relax to its equilibrium value $\hat{\mathbf{n}}_{\mathrm{el}}(x,z)$.

For LC material formed by $4-n-pentyl-4'-cyanobiphenyl$ (5CB) molecules, the range of existence of nematic phase is [10] [297–308.3] [K]. In this case, the

density of LC material was chosen as [10] $10^3 [\mathrm{kg/m^3}]$. The Frank elastic coefficients for 5CB LC phase, obtained experimentally, are [11]: $K_1 = 10.5$ and $K_3 = 13.8$, at $T = 300$ K, respectively. All values of $K_i (i = 1,3)$ are given in [pN]. The rotational and six Leslie coefficients for this LC material are (in [Pa s] [12]): $\gamma_1 \sim 0.069$, $\gamma_2 \sim -0.086$, $\alpha_1 \sim -0.0066$, $\alpha_2 \sim -0.079$, $\alpha_3 \sim -0.007$, $\alpha_4 \sim 0.072$, $\alpha_5 \sim 0.048$, and $\alpha_6 \sim -0.03$, respectively. The heat conductivity coefficients for 5CB LC phase parallel ($\lambda_\parallel$) and perpendicular ($\lambda_\perp$) to the director are (in [W/m K] [13]) 0.24 and 0.13, respectively. In the following we use the measured value of the specific heat [14] $C_p \sim 10^3$ [J/kg K], the calculated value of the LC-air surface tension [15,16] $\gamma \sim 0.02$ [N/m], and the value of the absorption coefficient α, for the infrared laser with the wavelength of 1061 [nm], which is equal to 8 [$\mathrm{m^{-1}}$] [17]. In our calculations the thickness $2d$ of the LC sample is equal to 10 [μm].

The set of parameters that is involved in Eqs. (12)–(17) has the following values: $\delta_1 \sim 10^{-3}$, $\delta_2 \sim 0.3$, $\delta_3 \sim 10^{-6}$, and $\delta_4 \sim 10^{-4}$. Taking into account that the dimensionless temperature χ should be in the range of [0.97–1.0], the parameters δ_5 can be estimated as $\delta_5 \sim 7.0$. This estimation of $\delta_5 = \frac{2\alpha}{\pi \omega^2} \frac{d^2}{\lambda_\perp T_{\mathrm{NI}}} O_0$ was made taking into account the fact that the duration of the laser pulse of power $\mathcal{Q}_0 \sim 0.5$ W, for the infrared laser with the wavelength of 1061 [nm], was $\tau_{\mathrm{in}} \sim 2.0$ μs.

Using the fact that $\delta_3 \ll 1$, Eq. (13) can be considerably simplified and takes the form

$$a_1 \psi_{zzzz} + a_2 \psi_{xzzz} + a_3 \psi_{xxzz} + a_4 \psi_{xxxz} + a_5 \psi_{xxxx} + a_6 \psi_{zzz}$$
$$+ a_7 \psi_{xzz} + a_8 \psi_{xxz} + a_9 \psi_{xxx} + a_{10} \psi_{zz}$$
$$+ a_{11} \psi_{xz} + a_{12} \psi_{zz} + \mathcal{F} = 0, \quad (19)$$

where $a_i (i = 1,...,12)$ and $\mathcal{F}$ are functions that have been defined in the Appendix.

III. EVOLUTION OF THE FREE LC-AIR INTERFACE, TEMPERATURE, AND VELOCITY UNDER THE INFLUENCE OF THE TEMPERATURE GRADIENT

The evolution of the free LC-air interface under the influence of the temperature gradient $\nabla \chi$, caused by the laser beam focused in the interior of the LC sample, is governed by Eqs. (12), (19), and (14), together with the boundary [Eqs. (15) and (16)] and the initial [Eq. (17)] conditions. The calculations have been carried out by using both the relaxation [18] and the sweep [19] methods. The initial distribution of the director field $\hat{\mathbf{n}}_{\mathrm{el}}(x,z)$ has been obtained from Eq. (12) by means of the relaxation method with $(\psi)_x = (\psi)_z = (\chi)_x = (\chi)_z = 0$, and with the boundary $(n_x)_{x=\pm 10, -1 \leqslant z \leqslant 1} = (n_x)_{z=1, -10 \leqslant x \leqslant 10} = 0$, $(n_x)_{z=-1, -10 \leqslant x \leqslant 10} = 1$, and initial $n_x = \frac{1-z}{2}$, for $-10 < x < 10$, and $n_x = 0$, for $x = \pm 10$, conditions. Having obtained the initial distribution of the director field $\hat{\mathbf{n}}_{\mathrm{el}}(x,z)$, the initial distribution of the temperature field $\chi(x,z,\Delta\tau)$, corresponding to the first time step $\Delta\tau$, has been obtained from Eq. (14), by means of the relaxation method with $(\psi)_x = (\psi)_z = 0$ and with the boundary and initial conditions in the form of Eqs. (15) and (16), for the case of the flat interface. Having obtained the initial distributions of the director and the
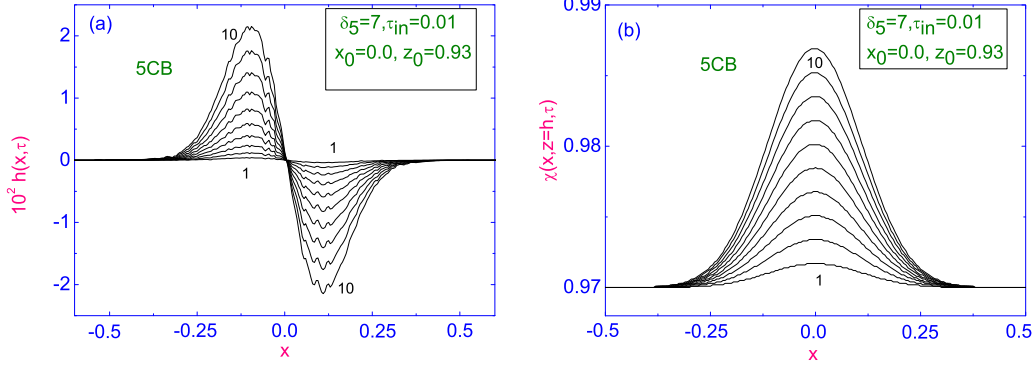
FIG. 1. (a) The evolution of both the dimensionless height $h(x,\tau)$ of the LC-air interface and the dimensionless temperature $\chi(x,\tau)$ (b) on the free LC-air interface Γ, during the heating regime with $\delta_5 = 7$ and $\tau_{in} = 0.01$, at different times $\tau_i = 2^i \times 10^{-5} (i = 1,...,10)$, respectively. The numbering of the curves increases from $i = 1$ to $i = 10$.

temperature fields, as well as the function $\mathcal{F}$, which is involved in Eq. (19), one can calculate, using Eq. (19), the initial distribution of the stream function $\psi(x,z,\Delta\tau)$, corresponding to the first time step $\Delta\tau$. The next time step $\Delta\tau$ for the velocity and temperature fields, as well as for the director 's distribution across the LC sample with the free flexible upper boundary is initiated by the sweep method. The stability of the numerical procedure for Eqs. (12), (14), and (19) was defined by the conditions [18]: $\frac{\Delta\tau}{\delta_3}(\frac{1}{(\Delta x)^2} + \frac{1}{(\Delta z)^2}) \leqslant \frac{1}{2}$, $\frac{3a_5}{(\Delta x)^4} - \frac{2a_1}{(\Delta z)^4} > 0$, where Δx and Δz are the space steps in the x and z directions, and a_1 and a_5 are the coefficients defined in Eq. (19). In the calculations, the relaxation criterion $\epsilon = |(\chi_{(m+1)}(x,z,\tau) - \chi_{(m)}(x,z,\tau))/\chi_{(m)}(x,z,\tau)|$ was chosen to be equal to 10^{-4}, and the numerical procedure was then carried out until a prescribed accuracy has been achieved. Here, m is the iteration number.

Recently, the laser-induced heating has been used to inject the energy $O(x,z,\tau) = \delta_5 \exp[-2\frac{(x-x_0)^2+(z-z_0)^2}{\Delta^2}]\mathcal{H}(\tau_{in} - \tau)$ in the interior of the LC sample [2,5], where δ_5 is the dimensionless heat flow coefficient, Δ is the Gaussian spot size, and τ_{in} is the duration of the energy injection into the LC sample. Note that the magnitude δ_5 and duration τ_{in} of the heat injection are restricted only by the nematic phase stability condition. In the following, the heating regime with $\delta_5 = 7$ will be considered.

This estimation of $\delta_5 = \frac{2\alpha}{\pi\omega^2} \frac{d^2}{\lambda_\perp T_{NI}} O_0$ was made taking into account the fact that the duration of the laser pulse of power $\mathcal{Q}_0 \sim 0.5$ W, for the infrared laser with the wavelength of 1061 nm, was $\tau_{in} \sim 2.0$ μs. Figure 1 shows the evolution of the dimensionless height $h(x,\tau) = H(x,\tau) - 1$ [Fig. 1(a)] of the LC-air interface and the evolution of the dimensionless temperature $\chi(x,\tau)$ [Fig. 1(b)] on the free LC-air interface Γ, during the heating regime when the laser beam is focused in the interior ($x = 0.0$ and $z = 0.93$) of the LC sample, at different times $\tau_i = 2^i \times 10^{-5} (i = 1,...,10)$, respectively, whereas Fig. 2 shows the evolution of the horizontal $u(x,\tau)$ [Fig. 2(a)] and vertical $w(x,\tau)$ [Fig. 2(b)] components of the vector $\mathbf{v} = u\hat{\mathbf{i}} + w\hat{\mathbf{k}}$ on the LC-air interface. According to our calculations, the evolution of the height $h(x,\tau)$ of the LC-air interface is characterized by the wavelike profile along the x axis ($-0.5 < x < 0.5$). At the final stage of the evolution process, for $\tau = \tau_{in}$, the highest value of $|h| \sim 2 \times 10^{-2}$ is reached in the vicinity of points $x \sim \pm0.125$, whereas the evolution of the temperature χ is characterized by symmetric profile of $\chi(x,\tau)_{x\in\Gamma}$ with respect to the middle point ($x = 0.0$) of the LC-air interface Γ [see Fig. 1(b)]. In that case, during the heat step $[\tau \sim \tau_{in} \sim 0.01(\sim 2 [\mu s])]$ the evolution of the temperature profile $\chi(x,\tau)_{x\in\Gamma}$ is characterized by its strong growth in the vicinity of the middle point $x = 0.0$, up to the highest
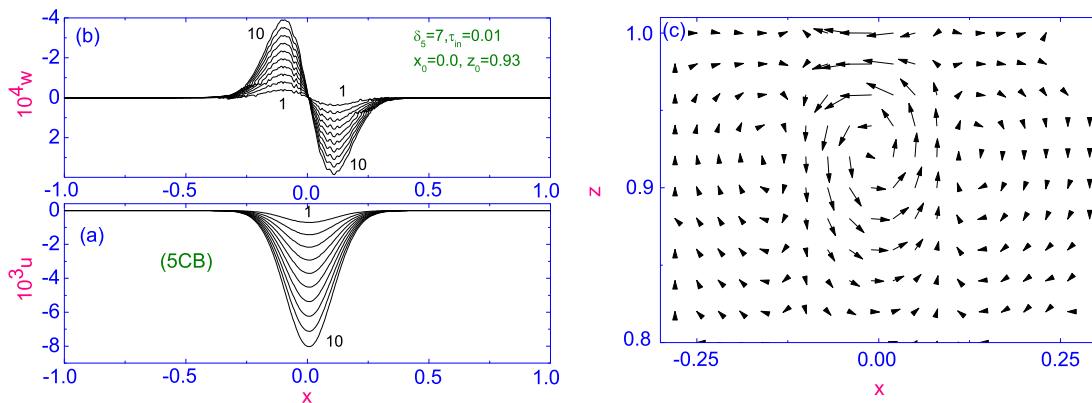
FIG. 2. Same as described in the caption of Fig. 1, but for evolution of both the horizontal $u(x,\tau)$ (a) and vertical $w(x,\tau)$ (b) components of the velocity vector $\mathbf{v} = u\hat{\mathbf{i}} + w\hat{\mathbf{k}}$ on the LC-air interface during the heating regime. (c) Distribution of the velocity field $\mathbf{v} = u\hat{\mathbf{i}} + w\hat{\mathbf{k}}$ in the LC sample after heating during $\tau = \tau_{in}$. Here 1 mm of the arrow length is equal to 0.4 μm/s.
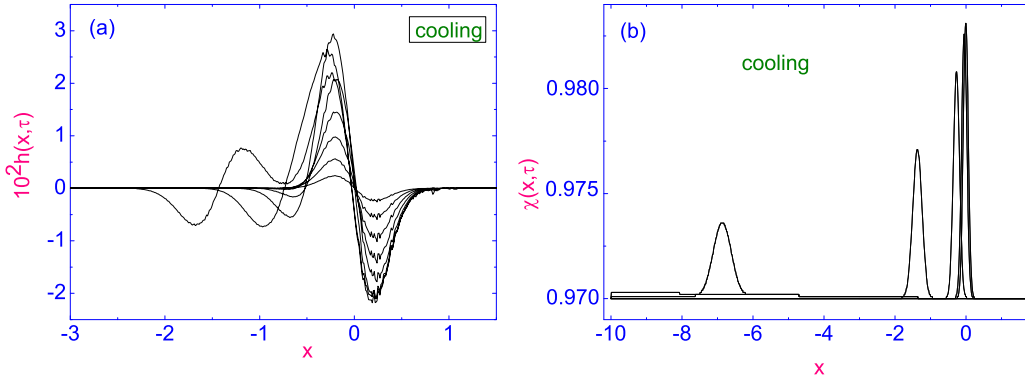
FIG. 3. The evolution of both the dimensionless height $h(x,\tau)$ (a) and the dimensionless temperature $\chi(x,\tau)$ (b) on the free LC-air interface Γ, during the cooling regime, at different times $\tau_i = 2^i \times 10^{-2} (i = 1,...,8)$, respectively.

value of 0.987 ($\sim$307 K), whereas the evolution of the dimensionless height h of the LC-air interface is characterized by two combs with the highest value of $|h| \sim 0.02 (\sim 0.01 \, [\mu m])$, which are directed in the opposite sense with respect to their center $x = 0.0$ [see Fig. 1(a)]. The thermally excited flow in that case is characterized by maintaining three vortices, one biggest vortical flow in the vicinity of the heat source initiated by the laser beam and directed in the negative sense (anticlockwise) around their center $x = 0.0, z \sim 0.93$, and two smallest vortices, which are settled down close to the points $x = \pm 0.13$ and $z \sim 0.93$, respectively [see Figs. 2(a)–2(c)]. According to our calculations the highest value of **v** on the LC-air interface is reached in the vicinity of the middle point $x = 0.0$. In that case, there is the biggest horizontal flow $u \sim 8 \times 10^{-3} (\sim 0.27 \, [\mu m/s])$ directed in the negative sense [see Fig. 2(a)], whereas the vertical flow w [see Fig. 2(b)] is characterized by very small value $\sim 4 \times 10^{-4} (\sim 13.2 \, [nm/s])$ directed in the opposite sense. Indeed, in the right-hand side of the LC sample, in the vicinity of the point $x \sim 0.125$, the vertical component $w \sim 4 \times 10^{-4} (\sim 13.2 \, [nm/s])$ of the vector **v** is directed in the positive sense, whereas in the left-hand side, in the vicinity of the point $x \sim -0.125$, the vertical component $w \sim 4 \times 10^{-4} (\sim 13.2 \, [nm/s])$ is directed in the negative sense. Our calculations also show that the range of distance z, counted from the lower solid boundary, over which the laser beam cannot disturb the nematic phase, is $0.8 \leqslant z \leqslant 1.0$, i.e., which is approximately 80% of the LC sample [see Fig. 2(c)]. Notice that the duration of the energy injection τ_{in} into the LC sample is restricted only by the nematic phase stability. Further calculations (cooling regime), based on the nonlinear extension of the Ericksen-Leslie theory, show that the LC material settles down to the rest during the time term $\tau_8 \sim 2.56 (\sim 0.5 \, [s])$, after switching off the laser power [see Fig. 3(a)], where both the horizontal u and vertical w components of the velocity **v** are equal to zero [see Figs. 4(a) and 4(b)], and the temperature field χ across the LC samples finally downfalls to the value on the lower and two lateral boundaries [see Fig. 3(b)]. Our calculations also show that the dimensionless height h and temperature χ profiles are shifted during the cooling regime, to the left-hand side of the LC sample. Such behavior of these profiles is caused by the existence of the horizontal flow directed in the negative sense. Figure 5 shows the distribution of the dimensionless

temperature $\chi(x,\tau)$ along the z axis ($0.7 \leqslant z \leqslant 1.0$), when the laser beam is focused in the center ($x = 0.0$) of the LC sample, but at different depths: (a) $z_0 = 0.98$, (b) $z_0 = 0.94$, (c) $z_0 = 0.90$, and $z_0 = 0.80$ (d), respectively. The heating regime when the laser beam is focused in the interior of the LC sample is given at different times $\tau_i = 2^i \times 10^{-5} (i = 6,...,10)$, respectively. It has been shown that as the focus of the laser beam is shifted in the depth of the LC sample, the temperature profiles across the LC sample does not undergo the crucial change. For instance, in the case when the laser beam is focused on the maximum depth ($z_0 = 0.8$), the heating does not reach the LC-air interface [see Fig. 5(d)]. In turn, the velocity profiles across the LC sample undergo the crucial change. Figure 6 shows the distribution of the horizontal $u(x = 0,z,\tau)$ and vertical $w(x = 0,z,\tau)$ components of the velocity vector **v** along the z axis ($0.7 \leqslant z \leqslant 1.0$), when the laser beam is focused in the center ($x = 0.0$) of the LC sample, but at different depths: (a) $z_0 = 0.98$, (b) $z_0 = 0.94$, (c) $z_0 = 0.90$, and $z_0 = 0.80$ (d), respectively. It has been shown that as the focus of the laser beam is shifted in the depth of the LC sample in the vicinity of the LC-air interface, the horizontal component of the velocity $u(x = 0,z,\tau)$ changes its direction from negative to positive, approximately at the point $x_0 = 0.0, z_0 \sim 0.9$, whereas the vertical component of
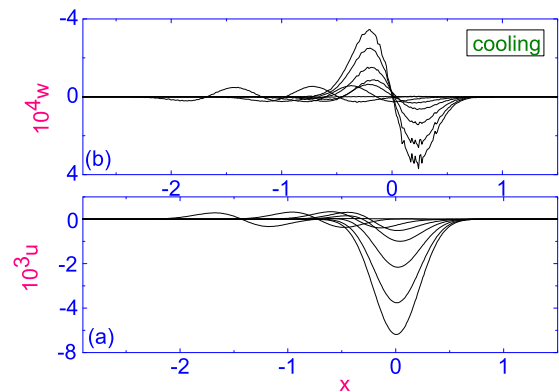
FIG. 4. The evolution of both the dimensionless horizontal $u(x,\tau)$ (a) and vertical $w(x,\tau)$ (b) components of the velocity field on the free LC-air interface Γ during the cooling regime, at different times $\tau_i = 2^i \times 10^{-2} (i = 1,...,8)$, respectively.
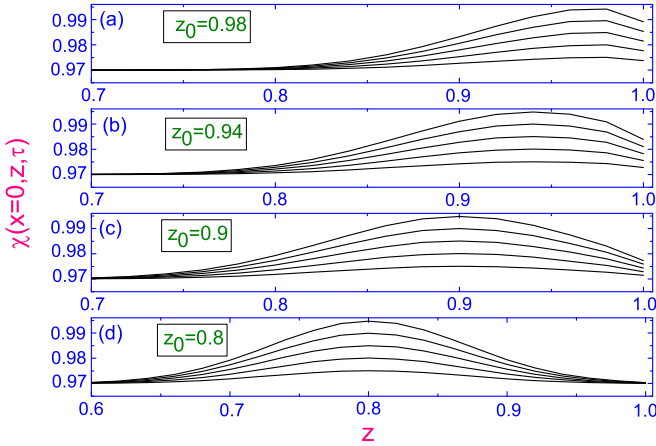
FIG. 5. Distribution of the dimensionless temperature $\chi(x=0,z,\tau)$ along the z axis ($0.6 \leqslant z \leqslant 1.0$), when the laser beam is focused in the center ($x=0.0$) of the LC sample, but at different depths: (a) $z_0 = 0.98$, (b) $z_0 = 0.94$, (c) $z_0 = 0.90$, and $z_0 = 0.80$ (d), respectively.

the velocity $w(x=0,z,\tau)$ rapidly drops to zero. It should be noted that the greatest value of $u(x=0,z,\tau)$, directed in the positive sense in the vicinity of the LC-air interface, achieved in the case when the laser beam is focused on the maximum depth of penetration ($z_0 = 0.8$) in the LC volume, whereas the greatest value of $u(x=0,z,\tau)$, directed in the negative sense in the vicinity of the LC-air interface, achieved in the case when the laser beam is focused on the minimum depth of penetration ($z_0 = 0.98$) in the LC volume. In both of these cases, the vertical component of the velocity vector $w(x=0,z,\tau)$ at the free LC-air interface is almost zero. So, this distribution of components of the velocity field shows that in the area close to the LC-air interface ($0.8 < z < 1.0$), due to pumping of energy by laser radiation, the vortical flow is excited similar to what is shown in Fig. 2(c). Our calculations also show that with further penetration of the injecting energy to the bulk of the LC phase, from $x_0 = 0.0$, $z_0 = 0.98$ to $x_0 = 0.0$, $z_0 = 0.8$, the thermally excited vortical flow changes the direction

from anticlockwise, around the point $x = 0.0$, $z = 0.98$, to clockwise, around the point $x = 0.0$, $z = 0.8$, approximately at the point $x_0 = 0.0$, $z_0 \sim 0.9$.

IV. CONCLUSION

In summary, we have investigated the reorientational dynamics in thin liquid crystal (LC) volume, where the nematic sample is confined in a microsized volume with a free flexible LC-air interface, under the influence of the temperature gradient ∇T, caused by a laser beam focused in the interior of the LC sample. Our calculations, based on the appropriate nonlinear extension of the classical Ericksen-Leslie theory, show that due to interaction between ∇T and the gradient of the director field $\nabla \hat{n}$, in the LC volume the thermally excited three-vortical fluid flow is maintained. The direction and magnitude of hydrodynamic flow, at a fixed time pumping energy and the laser output power, is influenced by depths of the laser injection. Our calculations also show that the range of distance, counted from the lower solid boundary, over which the laser beam cannot disturb the nematic phase, is approximately 80% of the LC sample.

Recently, the circular flow formation in homeotropically oriented LC film doped by chiral molecules has been observed [5]. It has been shown, by means of circular polarization techniques, that when the laser beam irradiation started, the thermocapillary flow from the laser spot position on the free LC interface to the radial outward direction occurred. After a while, the radial flow has turned into a circular flow. The formation of the circular flow on the top of the LC film has been ascribed to thermocapillary convection in the LC sample. In turn, in our case, the vortical flow is occurred in the vicinity of the free LC-air interface and penetrated to the bulk of the LC sample, and the mechanism that is responsible for occurring of the vortical flow near the LC-air interface is based on the coupling between director and temperature gradients, initiated by the laser beam irradiation. So, this vortical flow is a unique phenomena only exhibited by liquid crystal systems, and it is expected to be applied for optothermal tweezers.
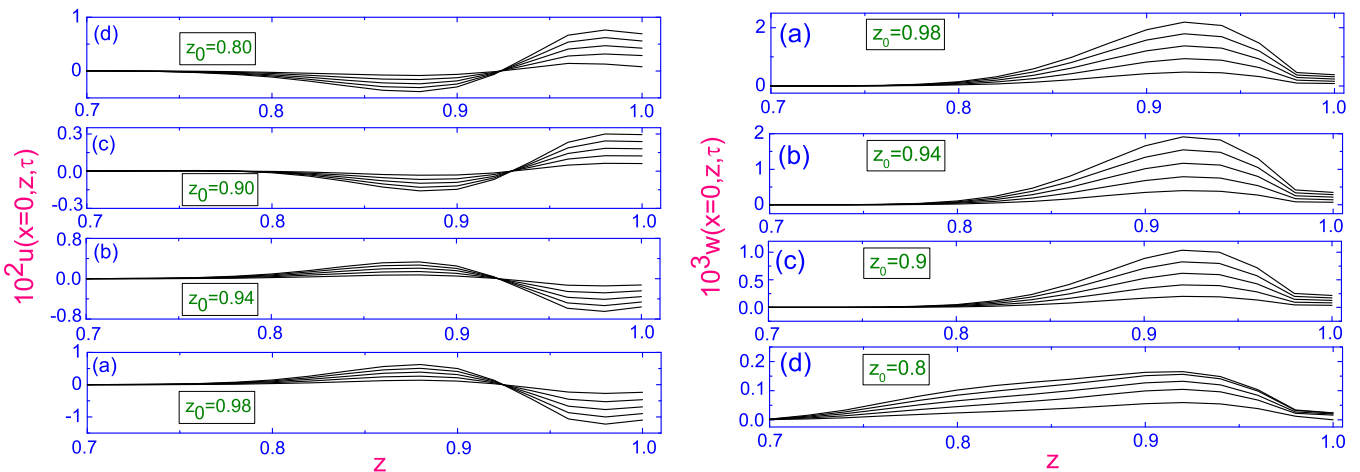
FIG. 6. Distribution of both the horizontal $u(x=0,z,\tau)$ and vertical $w(x=0,z,\tau)$ components of the velocity vector $\mathbf{v}$ along the z axis ($0.7 \leqslant z \leqslant 1.0$), when the laser beam is focused in the center ($x=0.0$) of the LC sample, but at different depths: (a) $z_0 = 0.98$, (b) $z_0 = 0.94$, (c) $z_0 = 0.90$, and $z_0 = 0.80$ (d), respectively.

APPENDIX: TORQUES AND STRESS TENSOR COMPONENTS

We believe that the present investigation can shed some light on the problem of control of the dynamic response of the LC display under the influence of the temperature gradient.

The torque balance equation can be derived from the dimension balance of elastic $\mathbf{T}_{el} = \frac{\delta \mathcal{W}_{el}}{\delta \hat{\mathbf{n}}} \times \hat{\mathbf{n}}$, viscous $\mathbf{T}_{vis} = \frac{\delta \mathcal{R}^{vis}}{\delta \hat{\mathbf{n}}_t} \times \hat{\mathbf{n}}$, and thermomechanical $\mathbf{T}_{tm} = \frac{\delta \mathcal{R}^{tm}}{\delta \hat{\mathbf{n}}_t} \times \hat{\mathbf{n}}$ torques, where $\mathcal{W}_{el} = \frac{1}{2}[K_1(\nabla \cdot \hat{\mathbf{n}})^2 + K_3(\hat{\mathbf{n}} \times \nabla \times \hat{\mathbf{n}})^2]$ is the elastic energy, and K_1 and K_3 are the splay and bend elastic coefficients, $\hat{\mathbf{n}}_t \equiv \frac{d\hat{\mathbf{n}}}{dt}$ is the material derivative of $\hat{\mathbf{n}} = n_x\hat{\mathbf{i}} + n_z\hat{\mathbf{k}}$, whereas $\mathcal{R}^{vis} = \alpha_1(\hat{\mathbf{n}} \cdot \mathbf{D}_s \cdot \hat{\mathbf{n}})^2 + \gamma_1(\hat{\mathbf{n}}_t - \mathbf{D}_a \cdot \hat{\mathbf{n}})^2 + 2\gamma_2(\hat{\mathbf{n}}_t - \mathbf{D}_a \cdot \hat{\mathbf{n}}) \cdot [\mathbf{D}_s \cdot \hat{\mathbf{n}} - (\hat{\mathbf{n}} \cdot \mathbf{D}_s \cdot \hat{\mathbf{n}})\hat{\mathbf{n}}] + \alpha_4 \mathbf{D}_s : \mathbf{D}_s + (\alpha_5 + \alpha_6)(\hat{\mathbf{n}} \cdot \mathbf{D}_s \cdot \mathbf{D}_s \cdot \hat{\mathbf{n}})$ is the viscous contribution to the total Rayleigh dissipation function $\mathcal{R} = \mathcal{R}^{vis} + \mathcal{R}^{tm} + \mathcal{R}^{th}$. Here, $\frac{1}{\xi}\mathcal{R}^{tm} = (\hat{\mathbf{n}} \cdot \nabla T)\mathbf{D}_s : \mathbf{M} + \nabla T \cdot \mathbf{D}_s \cdot \mathbf{M} \cdot \hat{\mathbf{n}} + (\hat{\mathbf{n}} \cdot \nabla T)[\hat{\mathbf{n}}_t - \mathbf{D}_a \cdot \hat{\mathbf{n}} - 3\mathbf{D}_s \cdot \hat{\mathbf{n}} + 3(\hat{\mathbf{n}} \cdot \mathbf{D}_s \cdot \hat{\mathbf{n}})\hat{\mathbf{n}}] \cdot \mathbf{M} \cdot \hat{\mathbf{n}} + \hat{\mathbf{n}}(\nabla \mathbf{v})^T \cdot \mathbf{M} \cdot \nabla T + \frac{1}{2}(\hat{\mathbf{n}} \cdot \mathbf{D}_s \cdot \hat{\mathbf{n}})\nabla T \cdot \mathbf{M} \cdot \hat{\mathbf{n}} + \hat{\mathbf{n}}_t \cdot \mathbf{M} \cdot \nabla T + \frac{1}{2}\mathcal{M}_0 \nabla T \cdot \nabla \mathbf{v} \cdot \hat{\mathbf{n}} + (\hat{\mathbf{n}} \cdot \nabla T)\mathcal{M}_0(\hat{\mathbf{n}} \cdot \mathbf{D}_s \cdot \hat{\mathbf{n}}) + \frac{1}{2}\mathcal{M}_0\hat{\mathbf{n}}_t \cdot \nabla T$, and $\mathcal{R}^{th} = \frac{1}{T}[\lambda_\parallel(\hat{\mathbf{n}} \cdot \nabla T)]^2 + \lambda_\perp[\nabla T - \hat{\mathbf{n}}(\hat{\mathbf{n}} \cdot \nabla T)^2]$ are

the thermomechanical and thermal contributions to $\mathcal{R}$, respectively. Here, $\alpha_1 \div \alpha_6$ are the Leslie viscosity coefficients, $\gamma_1(T)$ and $\gamma_2(T)$ are the rotational viscosity coefficients (RVCs), ξ is the thermomechanical constant, and $\lambda_\parallel$, $\lambda_\perp$ are the heat conductivity coefficients parallel and perpendicular to the director $\hat{\mathbf{n}}$, respectively. Here, $\mathbf{D}_s = \frac{1}{2}[\nabla \mathbf{v} + (\nabla \mathbf{v})^T]$ and $\mathbf{D}_a = \frac{1}{2}[\nabla \mathbf{v} - (\nabla \mathbf{v})^T]$ are the symmetric and asymmetric contributions to the rate of strain tensor, $\mathbf{M} = \frac{1}{2}[\nabla\hat{\mathbf{n}} + (\nabla\hat{\mathbf{n}})^T]$, and $\mathcal{M}_0 = \nabla \cdot \hat{\mathbf{n}}$ is the scalar invariant of the tensor $\mathbf{M}$. We use here the invariant, multiple dot convention: $\mathbf{ab} = a_ib_j$, $\mathbf{a} \cdot \mathbf{b} = a_ib_i$, $\mathbf{A} \cdot \mathbf{B} = A_{ik}B_{kj}$, and $\mathbf{A} : \mathbf{B} = A_{ik}B_{ki}$, where repeated Cartesian indices are summed.

The dimensionless elastic contribution to the torque balance equation is $T_{el} = n_z\mathcal{M}_{0,x} - n_x\mathcal{M}_{0,z} + K_{31}(n_z f_z + n_x f_x)$, whereas the dimensionless viscous and thermomechanical contributions are $T_{vis} = n_z n_{x,\tau} - n_x n_{z,\tau} + \frac{1}{2}\gamma_{21}(\psi_{zz} - \psi_{xx})(n_x^2 - n_z^2) - \frac{1}{2}(\psi_{zz} + \psi_{xx}) + 2\gamma_{21}\psi_{,xz}n_xn_z$ and $T_{tm} = \delta_2\chi_x(n_xn_{z,x} - \frac{3}{2}n_zn_{x,x} + \frac{1}{2}n_xn_{x,z}) + \delta_2\chi_z(-n_zn_{x,z} + \frac{3}{2}n_xn_{z,z} - \frac{1}{2}n_zn_{z,x})$, respectively. We consider the dimensionless elastic $\overline{\mathcal{W}}_{el}$ and dissipation $\overline{\mathcal{R}} = \overline{\mathcal{R}}_{vis} + \delta_2\overline{\mathcal{R}}_{tm} + \delta_3\overline{\mathcal{R}}_{th}$ functions as

$$\overline{\mathcal{W}}_{el} = n_z\mathcal{M}_{0,x} - n_x\mathcal{M}_{0,z} - \frac{K_3}{K_1}(n_z f_z - n_x f_x),$$

$$2\overline{\mathcal{R}}_{vis} = n_{x,\tau}^2 + n_{z,\tau}^2 + n_{x,\tau}[n_z(w_x - u_z) + 2\gamma n_x u_x + \gamma_{21}n_z(u_z + w_x)]$$

$$+ n_{z,\tau}[n_x(u_z - w_x) + 2\gamma n_z w_z + \gamma_{21}n_x(u_z + w_x)] + \frac{1}{\gamma_1}u_x^2[\alpha_4 + (\alpha_5 + \alpha_6)n_x^2 + \alpha_1 n_x^4]$$

$$+ \frac{1}{\gamma_1}w_z^2[\alpha_4 + (\alpha_5 + \alpha_6)n_z^2 + \alpha_1 n_z^4] + 2\frac{\alpha_1}{\gamma_1}u_x w_z n_x^2 n_z^2$$

$$+ \frac{1}{\gamma_1}u_z^2\left[\frac{\alpha_4}{2} + \frac{\gamma_1 + \alpha_5 + \alpha_6}{4} + \gamma_2(n_x^2 - n_z^2) + \alpha_1 n_x^2 n_z^2\right] + \frac{1}{\gamma_1}w_x^2\left[\frac{\alpha_4}{2} + \frac{\gamma_1 + \alpha_5 + \alpha_6}{4} + \gamma_2(n_z^2 - n_x^2) + \alpha_1 n_x^2 n_z^2\right]$$

$$+ \frac{1}{\gamma_1}u_z w_x\left[\alpha_4 + \frac{-\gamma_1 + \alpha_5 + \alpha_6}{2} + 2\alpha_1 n_x^2 n_z^2\right] + \frac{1}{\gamma_1}u_z u_x[-\gamma_2 n_x n_z + 2\alpha_1 n_x^3 n_z] + \frac{1}{\gamma_1}u_x w_x[\gamma_2 n_x n_z + 2\alpha_1 n_x^3 n_z]$$

$$+ \frac{1}{\gamma_1}u_z w_z[\gamma_2 n_x n_z + 2\alpha_1 n_x n_z^3] + \frac{1}{\gamma_1}w_z w_x[-\gamma_2 n_x n_z + 2\alpha_1 n_x n_z^3],$$

$$\overline{\mathcal{R}}_{tm} = \chi_x\left[-\frac{1}{2}n_z\mathcal{M}_0 - n_z M_{xx} + n_x^2(n_x M_{zz} - M_{xx}n_z + 2n_x M_{xz})\right]$$

$$+ \chi_z\left[\frac{1}{2}n_x\mathcal{M}_0 + n_x M_{zz} + n_z^2(n_x M_{zz} - M_{xx}n_x - 2n_z M_{xz})\right],$$

$$\overline{\mathcal{R}}_{th} = \frac{1}{\chi}[\lambda(\hat{\mathbf{n}} \cdot \nabla\chi)]^2 + [\nabla\chi - \hat{\mathbf{n}}(\hat{\mathbf{n}} \cdot \nabla\chi)^2],$$

where $f = n_{x,z} - n_{z,x}$, $f_x = \frac{\partial f}{\partial x}$, $\lambda = \frac{\lambda_\parallel}{\lambda_\perp}$.

The dimensionless stress tensor $\sigma = \sigma^{el} + \sigma^{vis} + \sigma^{tm} - P\mathcal{I}$ as the sum of elastic, viscous, thermomechanical parts and pressure can be obtained directly from the elastic contribution to the energy and Rayleigh dissipation function as $\sigma^{el} = -\frac{\partial \mathcal{W}_{el}}{\partial \nabla\hat{\mathbf{n}}} \cdot (\nabla\hat{\mathbf{n}})^T$, $\sigma^{vis} = \frac{\delta\mathcal{R}^{vis}}{\delta\nabla\mathbf{v}}$, and $\sigma^{tm} = \frac{\delta\mathcal{R}^{tm}}{\delta\nabla\mathbf{v}}$, for the elastic, viscous, and thermomechanical contributions, respectively. Straightforward calculations for the geometry $\hat{\mathbf{n}} = (n_x, 0, n_z)$ give the following expressions for the elastic σ_{ij}^{el}, viscous σ_{ij}^{vis}, and thermomechanical σ_{ij}^{tm} components of the ST, $i, j = x, z$:

$$\sigma_{xx}^{el} = \delta_1[-n_{x,x}\mathcal{M}_0 + K_{31}f n_{z,x}],$$

$$\sigma_{zz}^{el} = \delta_1[-n_{x,x}\mathcal{M}_0 + K_{31}f n_{z,z}],$$

$$\sigma_{xz}^{\text{el}} = \delta_1[-n_{x,x}\mathcal{M}_0 - K_{31}fn_{x,x}],$$

$$\sigma_{zx}^{\text{el}} = \delta_1[-n_{x,x}\mathcal{M}_0 - K_{31}fn_{x,z}],$$

$$\sigma_{xx}^{\text{vis}} = \gamma_{21}n_x\frac{dn_x}{dt} + \psi_{xz}\frac{1}{\gamma_1}\left[\alpha_4 + (\alpha_5 + \alpha_6)n_x^2 + \alpha_1 n_x^2(n_x^2 - n_z^2)\right] + \frac{\alpha_1}{\gamma_1}n_x^3 n_z(\psi_{zz} - \psi_{xx}) - \frac{1}{2}\gamma_{21}n_x n_z(\psi_{zz} + \psi_{xx}),$$

$$\sigma_{xz}^{\text{vis}} = \frac{1}{2}\left(n_z\frac{dn_x}{dt} - n_x\frac{dn_z}{dt}\right) + \frac{1}{2}\gamma_{21}\left(n_z\frac{dn_x}{dt} + n_x\frac{dn_z}{dt}\right) + \psi_{xz}\frac{1}{\gamma_1}\left[\alpha_1 n_x n_z(n_x^2 - n_z^2) + \gamma_2 n_x n_z\right]$$

$$+ \frac{1}{\gamma_1}(\psi_{zz} - \psi_{xx})\left[\alpha_1 n_x^2 n_z^2 + \frac{\alpha_4}{2} + \frac{\alpha_5 + \alpha_6}{4}\right] - \frac{1}{4}(\psi_{zz} + \psi_{xx}) + \frac{1}{2}\gamma_{21}\psi_{xx}(n_x^2 - n_z^2),$$

$$\sigma_{zx}^{\text{vis}} = \frac{1}{2}\left(n_x\frac{dn_z}{dt} - n_z\frac{dn_x}{dt}\right) + \frac{1}{2}\gamma_{21}\left(n_z\frac{dn_x}{dt} + n_x\frac{dn_z}{dt}\right) - \psi_{xz}\frac{1}{\gamma_1}\left[\alpha_1 n_x n_z(n_z^2 - n_x^2) + \gamma_2 n_x n_z\right]$$

$$+ \frac{1}{\gamma_1}(\psi_{zz} - \psi_{xx})\left[\alpha_1 n_x^2 n_z^2 + \frac{\alpha_4}{2} + \frac{\alpha_5 + \alpha_6}{4}\right] + \frac{1}{4}(\psi_{zz} + \psi_{xx}) + \frac{1}{2}\gamma_{21}\psi_{zz}(n_x^2 - n_z^2),$$

$$\sigma_{zz}^{\text{vis}} = \gamma_{21}n_z\frac{dn_z}{dt} - \psi_{xz}\frac{1}{\gamma_1}\left[\alpha_4 + (\alpha_5 + \alpha_6)n_z^2 + \alpha_1 n_z^2(n_z^2 - n_x^2)\right] + \alpha_1 n_z^3 n_x(\psi_{zz} - \psi_{xx}) + \frac{1}{2}\gamma_{21}n_x n_z(\psi_{zz} + \psi_{xx}),$$

$$\sigma_{xx}^{\text{tm}} = \delta_1\chi_x\left[\frac{1}{2}M_{xx}n_x(3n_x^2 + 7) + M_{xz}n_z\left(1 + \frac{7}{2}n_x^2\right) + M_{zz}n_x\left(\frac{3}{2} + 2n_z^2\right)\right]$$

$$+ \delta_1\chi_z\left[M_{xx}n_z(n_x^2 + 1) + \frac{1}{2}M_{xz}n_x(3 + 5n_z^2) + \frac{3}{2}M_{zz}n_z(1 + n_z^2)\right],$$

$$\sigma_{xz}^{\text{tm}} = \delta_1\chi_x\left[\frac{1}{2}M_{xx}n_z(n_x^2 + 3) + M_{xz}n_x\left(3n_z^2 - \frac{1}{2}\right) + M_{zz}n_z^3\right] + \delta_1\chi_z\left[\frac{1}{2}M_{xx}n_x - \frac{1}{2}M_{xz}n_z(3 - n_x^2) - \frac{1}{2}M_{zz}n_x n_z^2\right],$$

$$\sigma_{zx}^{\text{tm}} = \delta_1\chi_x\left[-\frac{1}{2}M_{xx}n_z n_x^2 + \frac{1}{2}M_{xz}n_x(3 - n_z^2) + \frac{1}{2}M_{zz}n_z\right] + \delta_1\chi_z\left[M_{xx}n_x^3 + \frac{1}{2}M_{xz}n_z(3n_x^2 - 1) + \frac{1}{2}M_{zz}n_x(1 + n_z^2)\right],$$

$$\sigma_{zz}^{\text{tm}} = \delta_1\chi_x\left[\frac{3}{2}M_{xx}n_x(n_x^2 + 1) + M_{xz}n_z(3 + 5n_x^2) + M_{zz}n_x(1 + n_z^2)\right]$$

$$+ \delta_1\chi_z\left[M_{xx}n_z\left(2n_x^2 + \frac{3}{2}\right) + M_{xz}n_x\left(1 + \frac{7}{2}n_z^2\right) + \frac{1}{2}M_{zz}n_z(7 + 3n_z^2)\right].$$

The biharmonic equation in the ST terms has the form

$$\delta_3\psi_{,xz\tau} = \left(\sigma_{xx}^{\text{vis}} - \sigma_{zz}^{\text{vis}}\right)_{xz} + \left(\sigma_{zx}^{\text{vis}}\right)_{zz} - \left(\sigma_{xz}^{\text{vis}}\right)_{xx} + \mathcal{F},$$

or

$$\delta_3\psi_{xz\tau} = a_1\psi_{zzzz} + a_2\psi_{xzzz} + a_3\psi_{xxzz} + a_4\psi_{xxxz} + a_5\psi_{xxxx} + a_6\psi_{zzz}$$

$$+ a_7\psi_{xzz} + a_8\psi_{xxz} + a_9\psi_{xxx} + a_{10}\psi_{zz} + a_{11}\psi_{xz} + a_{12}\psi_{xx} + \mathcal{F},$$

where $\mathcal{F} = (\sigma_{xx}^{\text{el}} + \sigma_{xx}^{\text{tm}} - \sigma_{zz}^{\text{el}} - \sigma_{zz}^{\text{tm}})_{xz} + (\sigma_{zx}^{\text{el}} + \sigma_{zx}^{\text{tm}})_{zz} - (\sigma_{xz}^{\text{el}} + \sigma_{xz}^{\text{tm}})_{xx}$, whereas the coefficients $a_i(i = 1,...,12)$ have the following elements:

$$a_1 = \frac{1}{2} + \frac{1}{\gamma_1}\left[\frac{\alpha_4}{2} + \frac{\alpha_5 + \alpha_6}{4} + \alpha_1 n_x^2 n_z^2\right] + \frac{\gamma_{21}}{2}(n_x^2 - n_z^2) - \frac{\gamma_{21}^2}{4}(n_x^2 - n_z^2)^2,$$

$$a_2 = -\frac{2}{\gamma_1}\left[\alpha_1 n_x n_z(n_z^2 - n_x^2) + \gamma_2 n_x n_z\right] + 2\gamma_{21}^2 n_x n_z(n_x^2 - n_z^2),$$

$$a_3 = 1 + \frac{1}{\gamma_1}\left[\alpha_4 + \frac{\alpha_5 + \alpha_6}{2} - \alpha_1(n_x^4 + n_z^4)\right] - 4\gamma_{21}^2 n_x^2 n_z^2 + \frac{1}{2}\gamma_{21}^2(n_x^2 - n_z^2),$$

$$a_4 = \frac{2}{\gamma_1}\left[\alpha_1 n_x n_z(n_z^2 - n_x^2) - \gamma_2 n_x n_z\right] - 2\gamma_{21}^2 n_x n_z(n_x^2 - n_z^2),$$

$$a_5 = \frac{1}{2} + \frac{1}{\gamma_1}\left[\frac{\alpha_4}{2} + \frac{\alpha_5 + \alpha_6}{4} + \alpha_1 n_x^2 n_z^2\right] - \frac{\gamma_{21}}{2}(n_x^2 - n_z^2) - \frac{\gamma_{21}^2}{4}(n_x^2 - n_z^2)^2,$$

$$a_6 = \frac{1}{\gamma_1}\left[\left(\alpha_1 + \frac{\gamma_2^2}{\gamma_1}\right)n_x n_z(n_x^2 - n_z^2) + 2\gamma_2 n_x n_z\right]_x + \frac{1}{\gamma_1}\left[\alpha_1 n_x^2 n_z^2 + \frac{\gamma_2}{2}(n_x^2 - n_z^2)\right]_z - \frac{\gamma_{21}^2}{4}[(n_x^2 - n_z^2)^2]_z,$$

$$a_7 = -\frac{2}{\gamma_1}\big[\alpha_1 n_x n_z(n_x^2 - n_z^2) + \gamma_2 n_x n_z\big]_z - \frac{1}{\gamma_1}\Big[\alpha_1(n_x^2 - n_z^2)^2 + 4\frac{\gamma_2^2}{\gamma_1}(n_x^2 n_z^2)\Big]_x + \frac{1}{4}\big[1 + \gamma_{21}(n_x^2 - n_z^2)\big]_x^2 + 2\gamma_{21}^2\big[n_x n_z(n_x^2 - n_z^2)\big]_z,$$

$$a_8 = \frac{1}{\gamma_1}\Big[\Big(-\alpha_1 + \frac{\gamma_2^2}{4\gamma_1}\Big)(n_z^2 - n_x^2)^2 - \Big(2\alpha_1 + \frac{4\gamma_2^2}{\gamma_1}\Big)n_x^2 n_z^2\Big]_z + \frac{2}{\gamma_1}\Big[\Big(\alpha_1 + \frac{\gamma_2^2}{\gamma_1}\Big)(n_z^2 - n_x^2)n_x n_z - \gamma_2 n_x n_z\Big]_x.$$

$$a_9 = \frac{1}{\gamma_1}\Big[-\Big(\alpha_1 + \frac{\gamma_2^2}{\gamma_1}\Big)n_x n_z(n_x^2 - n_z^2) - 2\gamma_2 n_x n_z\Big]_z + \frac{1}{\gamma_1}\Big[\alpha_1 n_x^2 n_z^2 - \frac{\gamma_2}{2}(n_x^2 - n_z^2)\Big]_x - \frac{\gamma_{21}^2}{4}\big[(n_x^2 - n_z^2)^2\big]_x,$$

$$a_{10} = \frac{1}{\gamma_1}\Big[\alpha_1 n_x^2 n_z^2 + \frac{3\gamma_2}{4}(n_x^2 - n_z^2)\Big]_{zz} - \frac{1}{\gamma_1}\Big[\alpha_1 n_x^2 n_z^2 + \frac{\gamma_2}{4}(n_x^2 - n_z^2)\Big]_{xx} + \frac{\gamma_{21}}{4}(n_x^2 - n_z^2)\big[(n_x^2 - n_z^2)_{xx} - 2(n_x^2 - n_z^2)_{zz}\big]$$
$$- \Big[\frac{\alpha_1}{\gamma_1}n_x n_z(n_z^2 - n_x^2) - \gamma_{21}n_x n_z\Big]_{xz} + \gamma_{21}^2 n_x n_z(n_x^2 - n_z^2)_{xz} + \gamma_{21}^2\big[(n_x n_z)_x(n_x^2 - n_z^2)_z + (n_x n_z)_z(n_x^2 - n_z^2)_x\big]$$
$$- \gamma_{21}^2\Big[\frac{1}{4}\big((n_x^2 - n_z^2)_z\big)^2 - \frac{1}{4}\big((n_x^2 - n_z^2)_x\big)^2\Big],$$

$$a_{11} = -\frac{1}{\gamma_1}\big[\alpha_1 n_x n_z(n_x^2 - n_z^2)\big]_{xx} - \frac{1}{\gamma_1}\big[\alpha_1 n_x n_z(n_x^2 - n_z^2)\big]_{zz} - \frac{\alpha_1}{\gamma_1}\big[(n_x^2 - n_z^2)^2\big]_{xz}$$
$$- \gamma_{21}^2\big[n_x n_z(n_z^2 - n_x^2)_{zz} + (n_x n_z)_{zz}(n_x^2 - n_z^2) - n_x n_z(n_z^2 - n_x^2)_{xx} + (n_x n_z)_{xx}(n_x^2 - n_z^2)\big]$$
$$+ \gamma_{21}^2\big[8 n_x n_z(n_z n_x)_{xz} + 8(n_z n_x)_z(n_z n_x)_x + (n_z n_x)_z(n_x^2 - n_z^2)_x + (n_z n_x)_x(n_x^2 - n_z^2)_x\big],$$

$$a_{12} = \frac{1}{\gamma_1}\Big[\alpha_1 n_x^2 n_z^2 - \frac{3\gamma_2}{4}(n_x^2 - n_z^2)\Big]_{xx} + \frac{1}{\gamma_1}\Big[\alpha_1 n_x^2 n_z^2 + \frac{\gamma_2}{4}(n_x^2 - n_z^2)\Big]_{zz} + \frac{\gamma_{21}^2}{4}(n_x^2 - n_z^2)\big[(n_x^2 - n_z^2)_{zz} - 2(n_x^2 - n_z^2)_{xx}\big]$$
$$- \Big[\frac{\alpha_1}{\gamma_1}n_x n_z(n_z^2 - n_x^2) - \gamma_{21}n_x n_z\Big]_{xz} - \gamma_{21}(n_x n_z)_{xz}\big[1 + \gamma_{21}(n_x^2 - n_z^2)\big] - \gamma_{21}^2 n_x n_z(n_x^2 - n_z^2)_{xz}$$
$$- \gamma_{21}^2\big[(n_x n_z)_z(n_x^2 - n_z^2)_x + (n_x n_z)_x(n_x^2 - n_z^2)_x\big] - \frac{\gamma_{21}^2}{4}\big\{\big[(n_x^2 - n_z^2)_z\big]^2 - \big[(n_x^2 - n_z^2)_x\big]^2\big\}.$$

The dimensionless analog of the heat current $\mathbf{q} = -T\frac{\partial \mathcal{R}}{\partial \nabla T}$ is given by

$$-q_x = \chi_{,x}\big(\Lambda n_x^2 + n_z^2\big) + (\Lambda - 1)n_x n_z \chi_{,z} + \delta_4 \nabla_x\Big(\chi\frac{\partial \mathcal{R}^{\text{tm}}}{\partial \nabla \chi}\Big),$$

$$-q_z = \chi_{,z}\big(\Lambda n_z^2 + n_x^2\big) + (\Lambda - 1)n_x n_z \chi_{,x} + \delta_4 \nabla_z\Big(\chi\frac{\partial \mathcal{R}^{\text{tm}}}{\partial \nabla \chi}\Big),$$

whereas the dimensionless entropy balance equation can be rewritten in the form

$$\chi_{,\tau} = \big[\chi_{,x}\big(\Lambda n_x^2 + n_z^2\big) + (\Lambda - 1)n_x n_z \chi_{,z}\big] + \big[\chi_{,z}\big(\Lambda n_z^2 + n_x^2\big) + (\Lambda - 1)n_x n_z \chi_{,x}\big]$$
$$+ \delta_4 \chi\Big(\nabla \cdot \frac{\partial \mathcal{R}^{\text{tm}}}{\partial \nabla \chi}\Big) + \delta_5 O(x, z, \tau) - \psi_z \chi_x + \psi_x \chi_z.$$

The matrix equation

$$\hat{\mathcal{B}} \cdot \vec{\Psi} = \vec{\mathcal{C}},$$

for the vector $\vec{\Psi} = (\psi_{xx}, \psi_{xz}, \psi_{zz})$ can be obtained from Eqs. (5), (6), and (12), transmitted to the LC-air interface, where the matrix $\hat{\mathcal{B}}_{ij} \equiv b_{ij}(i, j = 1,2,3)$ has the following elements:

$$b_{11} = (n_x)_{z=h}\Big(2\gamma_{21} - \gamma_{21}^2 + \frac{2\alpha_4 + \alpha_5 + \alpha_6 - 2\alpha_1}{2\gamma_1}\Big),$$

$$b_{12} = -\frac{\alpha_4 + \alpha_5 + \alpha_6 + \alpha_1}{\gamma_1},$$

$$b_{13} = (n_x)_{z=h}\Big(\gamma_{21} + \gamma_{21}^2 - \frac{2\alpha_4 + \alpha_5 + \alpha_6 + 2\alpha_1}{2\gamma_1}\Big),$$

$$b_{21} = \frac{1}{4} - \frac{2\alpha_4 + \alpha_5 + \alpha_6}{4\gamma_1},$$

$$b_{22} = (n_x)_{z=h}\left(-\gamma_{21}^2 - \frac{2\alpha_4 + \alpha_5 + \alpha_6 + 2\alpha_1}{\gamma_1}\right),$$

$$b_{23} = \frac{1}{2} - \frac{\gamma_{21}}{2} - \frac{\gamma_{21}^2}{4} + \frac{2\alpha_4 + \alpha_5 + \alpha_6}{4\gamma_1},$$

$$b_{31} = \frac{\gamma_{21} - 1}{2},$$

$$b_{32} = -2\gamma_{21}(n_x)_{z=h},$$

$$b_{33} = -\frac{\gamma_{21} + 1}{2}$$

whereas the vector $\vec{\mathcal{C}} = (c_1, c_2, c_3)$ has the following elements:

$$c_1 = 2\gamma(n_{x,x})_{z=h} - \mathcal{P},$$

$$c_2 = \frac{\delta_1}{2}(\gamma_{21} - 1)[3\chi_x(n_{x,x})_{z=h} + \chi_z(n_{x,z})_{z=h}],$$

$$c_3 = \delta_1\left(\frac{3}{2}\chi_x(n_{x,x})_{z=h} + \chi_z(n_{x,z})_{z=h}\right).$$

Here, $\mathcal{P} = \frac{d^2}{K_1}P$ is the dimensionless pressure acting on the interface and γ is the dimensionless surface tension.

---

[1] A. D. Rey, Soft Matter **6**, 3402 (2010).

[2] E. Verneuil, M. L. Cordero, F. Gallaire, and C. Baroud, Langmuir **25**, 5127 (2009).

[3] A. V. Zakharov, A. A. Vakulenko, and M. Iwamoto, J. Chem. Phys. **132**, 224906 (2010).

[4] A. V. Zakharov and A. A. Vakulenko, Phys. Fluids **25**, 113101 (2013).

[5] H. Choi and H. Takezoe, Soft Matt. **12**, 481 (2016).

[6] J. L. Ericksen, Arch. Ration. Mech. Anal. **4**, 231 (1960).

[7] F. M. Leslie, Arch. Ration. Mech. Anal. **28**, 265 (1968).

[8] L. D. Landau and E. M. Lifshitz, *Fluid Mechanics* (Pergamon Press, Oxford, 1987).

[9] R. S. Akopyan and B. Y. Zeldovich, JETP **60**, 953 (1984).

[10] W. H. de Jeu, *Physical Properties of Liquid Crystal Materials* (Gordon and Breach, New York, 1980).

[11] N. V. Madhusudana and R. B. Ratibha, Mol. Cryst. Liq. Cryst. **89**, 249 (1982).

[12] A. G. Chmielewski, Mol. Cryst. Liq. Cryst. **132**, 339 (1986).

[13] M. Marinelli, A. K. Ghosh, and F. Mercuri, Phys. Rev. E **63**, 061713 (2001).

[14] P. Jamee, G. Pitsi, and J. Thoen, Phys. Rev. E **66**, 021707 (2002).

[15] A. V. Zakharov and A. A. Vakunenko, Phys. Rev. E **86**, 031701 (2012).

[16] A. V. Zakharov and I. Sliwa, J. Chem. Phys. **140**, 124705 (2014).

[17] I.-C. Khoo and S.-T. Wu, *Optics and Nonlinear Optics of Liquid Crystal* (World Scientific, Singapure, 1993), p. 59.

[18] I. S. Berezin and N. P. Zhidkov, *Computing Methods*, 4th ed. (Pergamon Press, Oxford, 1965).

[19] A. A. Samarskij and E. S. Nikolaev, *Numerical Method for Grid Equations* (Birkhauser, Basel, 1988), p. 284.